International Academic Institute for Science and Technology

International Academic Journal of Science and Engineering
Vol. 9, No. 2, 2022, pp. 66-73.

ISSN 2454-3896

International Academic Journal of Science and Engineering

www.iaiest.com

The Influence of Increasing Argon Gas Flow Rate on Plasma Parameters and their Diagnostics by Optical Emission Spectroscopy (OES)

Tamara Abood [a], Hammad Raheem [b], Layla Foad Ali [c]

[a] *Department of Physics, College of Science, University of Baghdad, Iraq.*
E-mail: tamara.aboud1104a@sc.uobaghdad.edu.iq
[b] *Department of Physics, College of Science, University of Baghdad, Iraq. E-mail: dr.hammad6000@yahoo.com*
[c] *Department of Biology, College of Science, University of Baghdad, Iraq.*

Abstract

In this research, the plasma parameters were determined each of electron temperature (T_e), electron density (n_e), plasma frequency (f_p), Debye length (λ_D). The plasma jet operates with argon gas at atmospheric pressure. It is equipped with an alternating AC high voltage power supply of 12 kilovolts and a frequency of 20 kilohertz. Plasma parameters were calculated from the emission spectrum using an optical emission spectrometer (OES) which captured the spectrum resulting from the plasma at various flow rates of argon gas from 0.5 to 5 L/min. Several peaks of argon gas (ArI) and nitrogen gas (N_2) were appeared, where the results showed that the highest peak of argon gas was at 763.51 nm for the fifth flow of argon gas. The results indicated the electron temperature (T_e) decrease with increased flow rate and ranged (1.296–0.645) ev, while the electron density (n_e) increased with flow rate and ranged were ($4.054\text{-}5.068 \times 10^{17}$) cm^{-3}, respectively. In contrast an increase in the intensity of spectral lines was observed.

Keywords: Optical Emission Spectroscopy, Electron Density, Voltage Power Supply.

DOI: 10.9756/IAJSE/V9I2/IAJSE0916
Received: 22 March 2022/Revised: 27 April 2022/Accepted: 27 May 2022/Published: 30 June 2022

Introduction

Atmospheric Cold Plasma (ACP), a substitute method for removing spoilage micro-organisms and pathogens from the contaminated objects, which include processed and fresh food surfaces, and medical devices, had received more attention in recent years among innovative non-thermal technologies. It has many benefits over traditional procedures, including nontoxic nature, quick treatment at low temperatures, and inexpensive operational costs [1,2]. The plasma jet is a promising method for producing cold, atmospheric pressure glow plasma. Due to their low masses, the electrons in the plasma jet are immediately affected by the external electric field. Many plasma processing processes mainly employ cold atmospheric pressure plasma, including the surface modification of various materials, medical applications, air treatment, water treatment, and gas treatment [3].

Additionally, because they cannot transfer a significant portion of their kinetic energy to the heavy particles, they have more considerable average kinetic energies than the latter. The initial reactions in the hierarchy of chemical kinetics are accounted for by electron-impact dissociation, excitation, and ionization. The other chemical reactions between the heavy particles are then started. ionization. The other chemical reactions between the heavy particles are then started. The electron density in the active plasma volume must be established because electron collisions are crucial to the plasma-chemical kinetics [4,5]. The Boltzmann plot is a powerful, straightforward, and frequently employed technique for measuring spectroscopy, particularly for determining electron temperature of plasma by comparing relative intensities of two or more line spectra with a significant difference of the energy. However, the excitation level needs to be obtained under a local thermal equilibrium (LTE) condition to use the Boltzmann plot method for practically measuring electron temperature [6]. The Boltzmann equation is described like follows:

$$ln\left[\frac{\lambda_{ji} I_{ji}}{hcA_{ji} g_j}\right] = -\frac{1}{KT}\left(E_j\right) + ln\left|\frac{N}{U(T)}\right| \qquad (1)$$

Where I_{ji} is relative emission line density between the I and j energy levels.

λ_{ji} represents Wave-length (in nm).

g_j is degeneracy or Statistical weight of upper level that has been emitted from transition phase.

A_{ji} represents possibility of the automatic radiation transmission from the level i to lower level j.

E_j is the energy of the excitation (in eV) for level i.

k represents Boltzmann constant.

N Densities of state population.

One of the most crucial aspects of gas discharges is the electron density, and plasma diagnostics are crucial for comprehending discharge physics and optimizing discharges. It is feasible to simultaneously assess electron density and temperature in cold Argon plasma jet through the analysis of Stark broadening of 2 distinct lines of emission. This method is based on the finding that various lines' Stark broadenings differ depending upon temperature and electron density. By comparing at least two line broadenings, we may therefore diagnose the electron density and temperature at same time [7,8]. Common methods for calculating the electron density include the Laser heterodyne interferometry, Langmuir probe, Laser Thomson scattering, and OES. Due to the small discharge size and robust collision processes, the probe method can't be utilized for the determination of non-thermal air pressure plasmas' electron density. The intricate and pricey laser setup further constrains the use of laser diagnostics in practical applications. OES, on the other hand, is popular in scientific and applied research and is simple, practical, and affordable [9]. Thus, the formula [10, 11] can be used to calculate the electron density.

$$n_e = \left[\frac{\Delta\lambda}{2\omega_s}\right] N_r \qquad (2)$$

Where $\Delta\lambda$ represents FWHM of the line, N_r represents reference electron density, and ω_s represents Stark broadening parameter which is found in standard tables.

In this study, Ar plasma is defined in terms of argon percent and operational parameters, the system operates at atmospheric pressure at a standard frequency of 20 kHz. By using the optical emission spectroscopy (OES) technique, was used to determine the characteristics of the atmospheric-pressure plasma jet. The electron temperature, which effects plasma reactivity via inelastic collisions, is calculated using the Boltzmann plot method from ArI spectral line intensities.

Experimental Work

1. Plasma Jet Configuration

The APPJs is shown in figure (1). The system consists of an AC alternating power supply consisting of two high voltage electrodes and the other grounded. The high voltage is connected to Pyrex glass tube surrounded by aluminum foil (10 mm) wide and (10 mm) away from its end. The aluminum foil is connected to a (12 kV) peak to peak the high-voltage power source generates a high voltage in the form of a sinusoidal waveform and a frequency of 20 kHz., where argon gas was used to generate plasma, a specific values of gas were controlled from (0.5 to 5) *l/min* using a flow meter where the gas flow starts from the argon gas bottle and then It moves to the gas regulator and through it the amount of gas outside is controlled, as the outside part is connected to an Pyrex glass tube. The diagnosis is collected by using a PC system for recording spectrum data, where the data wire is connected to the PC control, then the fiber optic is installed at an angle of 45^0 and at a distance of 1 cm from the tip of plasma jet. The data was recorded by changing the gas flow rate (0.5-5) *l/min.*

2. Optical Emission Spectroscopy (OES)

The active species in the plasma jet emission spectra were determined in the laboratory from the spectra obtained in the range (of 300-1000) nm. The OES was measured by spectrophotometer.

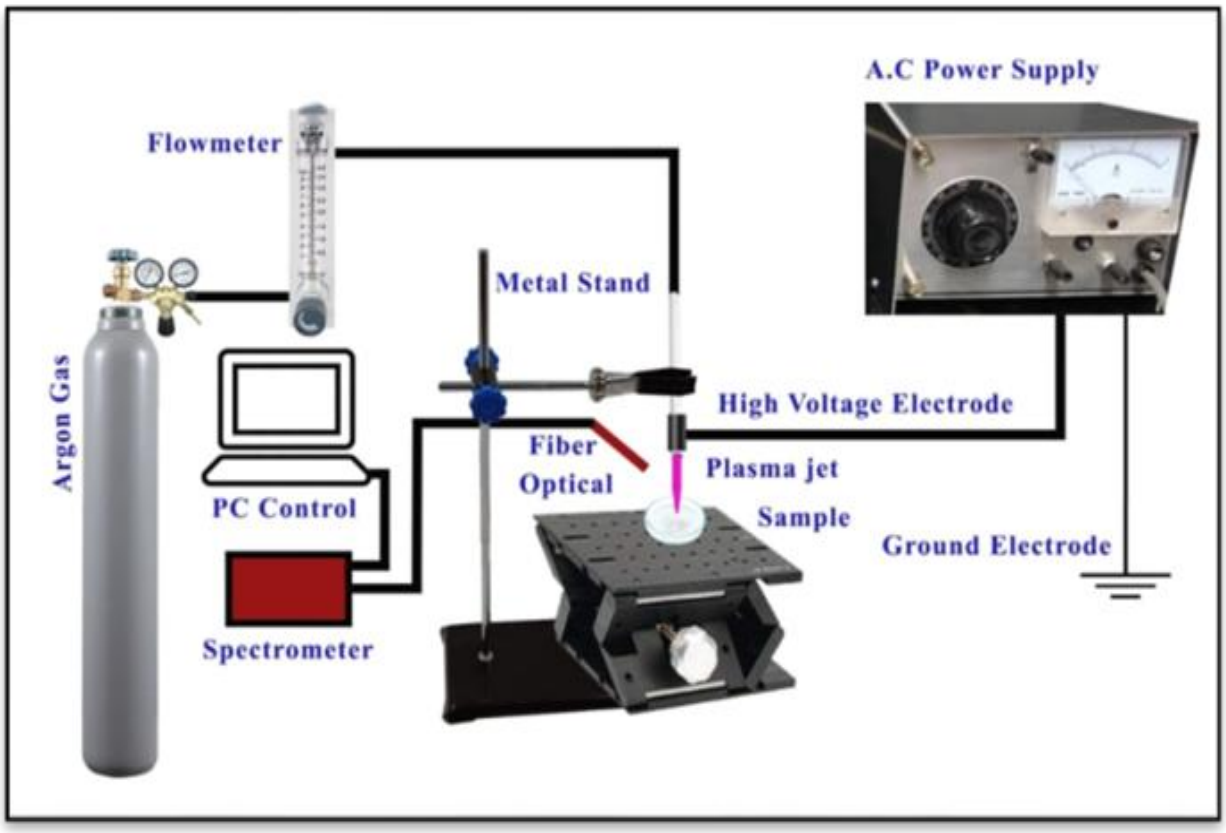


Figure 1: Setup of Diagnostic Spectroscopy of Non-thermal Atmospheric Pressure Plasma Jet

Results and Discussion

For varied values of gas flow rate (0.50, 1, 1.50, 2,2.5,3,3.5,4,4.5 and 5) l/min, the applied voltage was 12 kV, the current was 5 mA, the frequency was 20 kHz, the distance was 3 cm, and figure 3 shows the intensity distribution of the plasma spectrum as measured by OES.

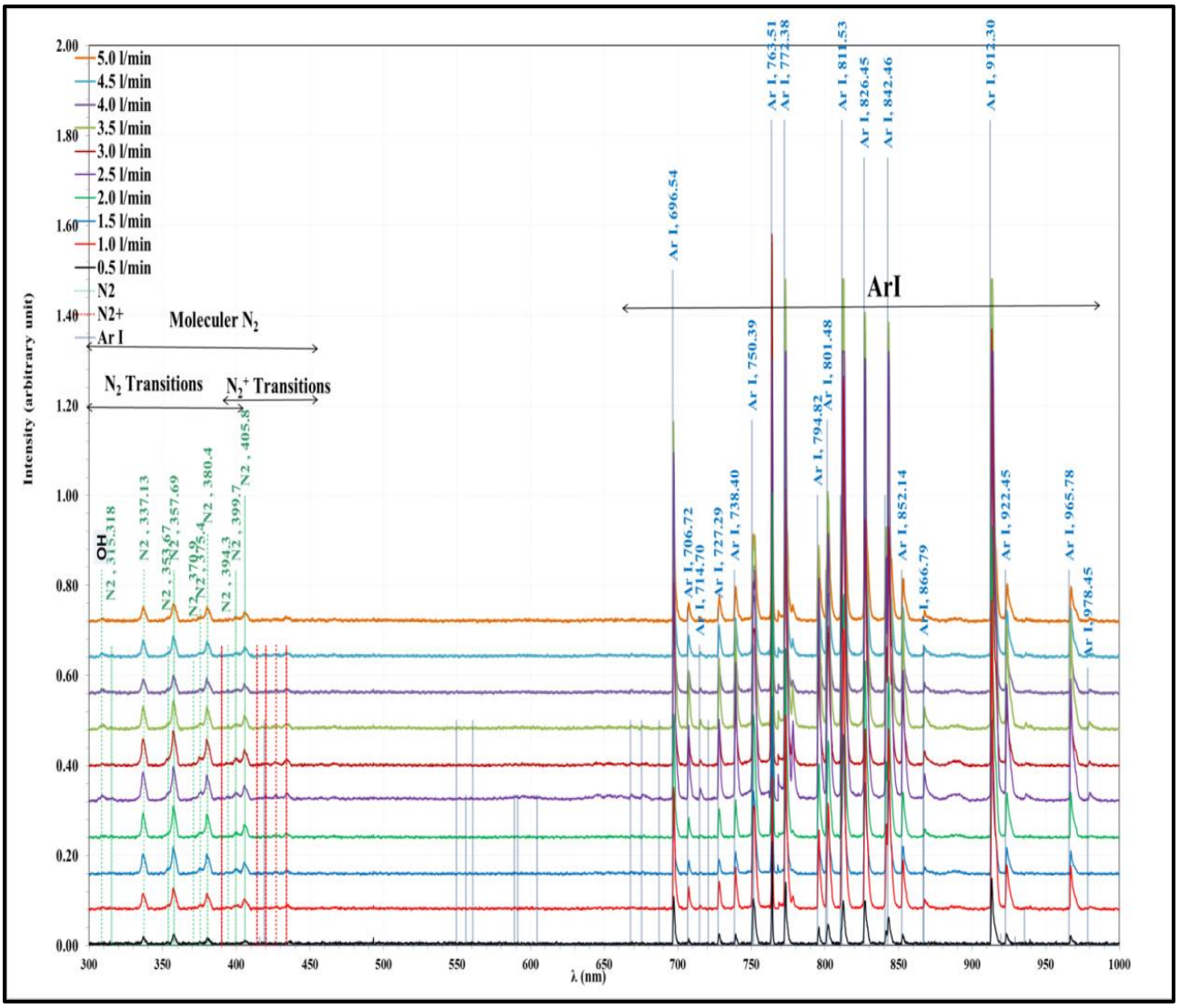


Figure 2: The Intensity Spectra of the APPJs with a Different Gas Flow Rate

The figure has numerous peaks, most of which are from the ArI and consistent with the NIST data [7]. Weak peaks for ArII can be seen in this spectrum. Depending upon gas flow rate, the highest peak can be seen at 763.51 nm. Which denotes the ArI-represented active species produced in the Argon plasma, which is consistent with [10]. Peaks in the visible range (300-1000 nm) were all found. Additionally, the same figure shows how height and sharpness increase peak as gas flow rate increases. For the highest peak, as shown in Fig. 3, it is seen that the peak intensity increases with the gas flow rate, which indicates an increase in the emission of the ArI species in the Argon plasma. There is a slight decrease in intensity at high gas flow rates, which may be caused by plasma ionization saturation. Additionally, when the gas flow rate increases, the peak half width decreases. The slope of the linear fitting of the result curve that is shown in Fig. 4 using eq ($slope = m = -\frac{1}{KT}$) might be used to compute the electron temperature at the highest peak and by plotting Ln $\left(\frac{I_{ji}\lambda_{ji}}{A_{ji}\, g_j}\right)$ Verses (E_j).

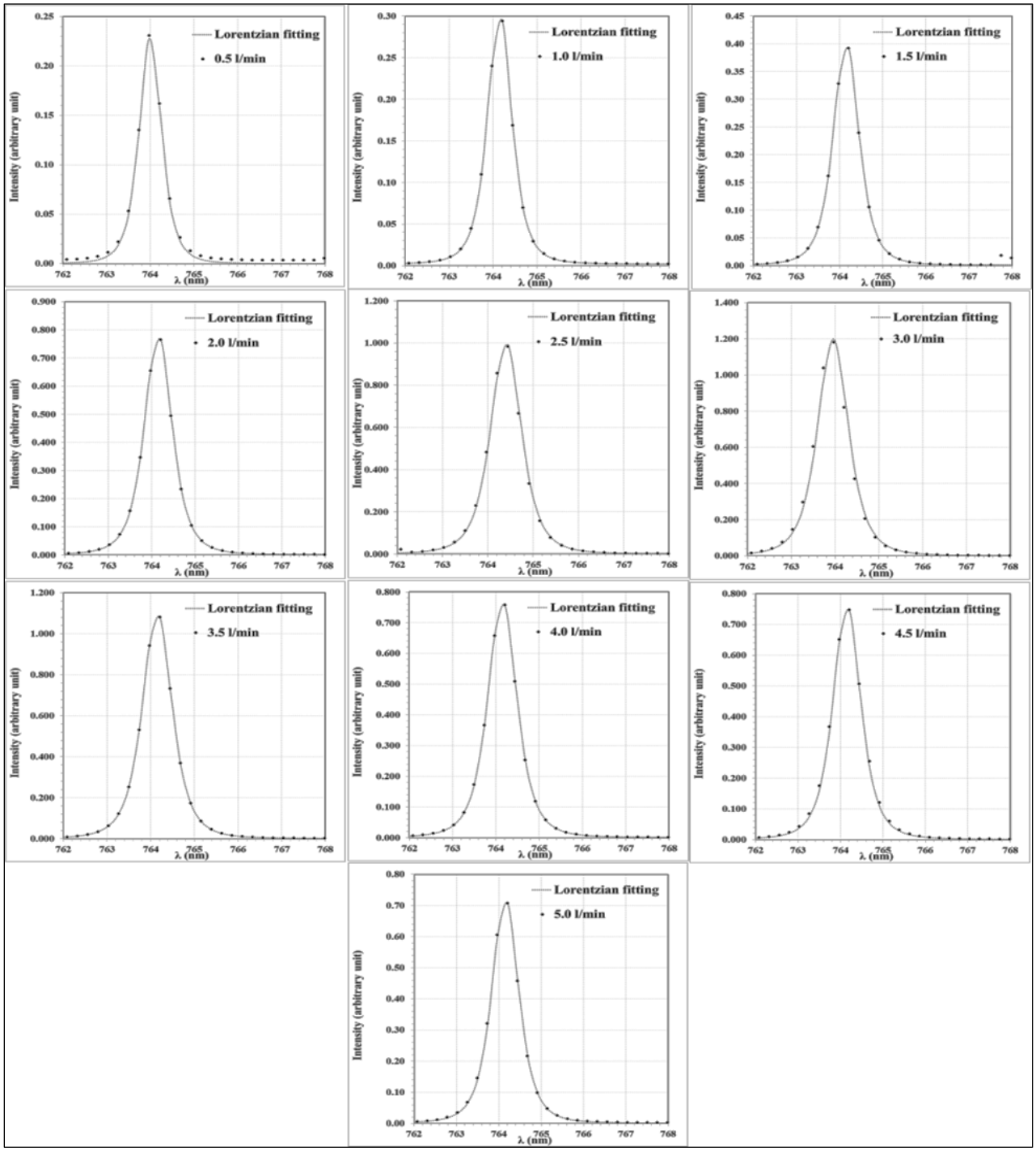


Figure 3: Stark-Broadening and Lorentzian Fitting for the line 746nm for different AR Gas Flow Rates

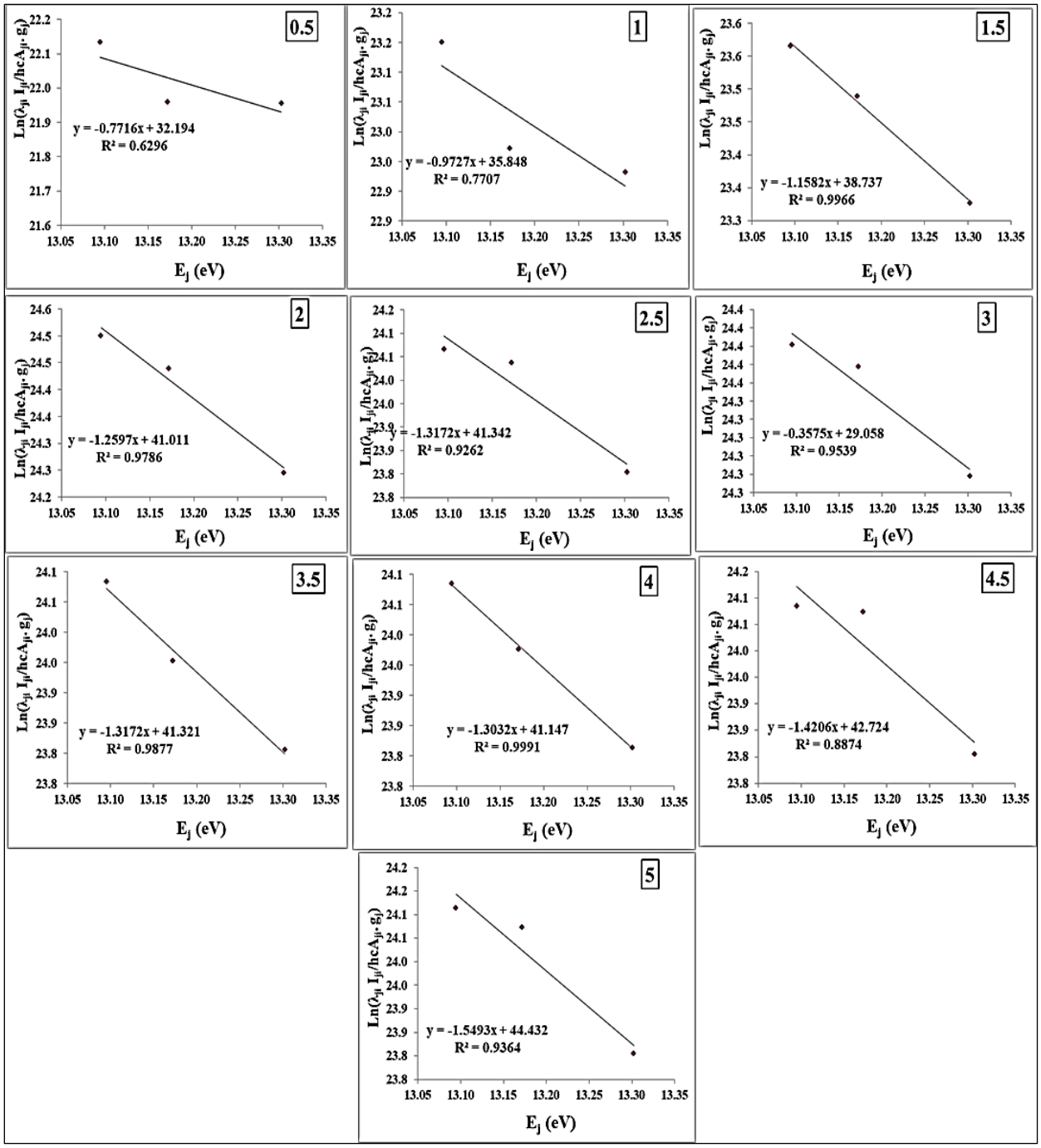


Figure 4: A Boltzmann Plot for Different Ar Gas Flow Rates Values

Electron temperature T_e, which is related to the slope of linear fitting by applying Eq ($slope = m = -\frac{1}{KT}$, is plotted on the vertical axis with E_j on the horizontal axis, hence, using Eq(2), it is possible to compute the electron density. Thus, we can explain the conclusions in Fig. 3. Figure (5) shows how such temperature and density of electrons change as a function of gas flow rate. This figure shows a decrease in electron temperature as gas flow rate increases. It also shows an increase in plasma jet electron density as gas flow rate increases. These results supported [7].

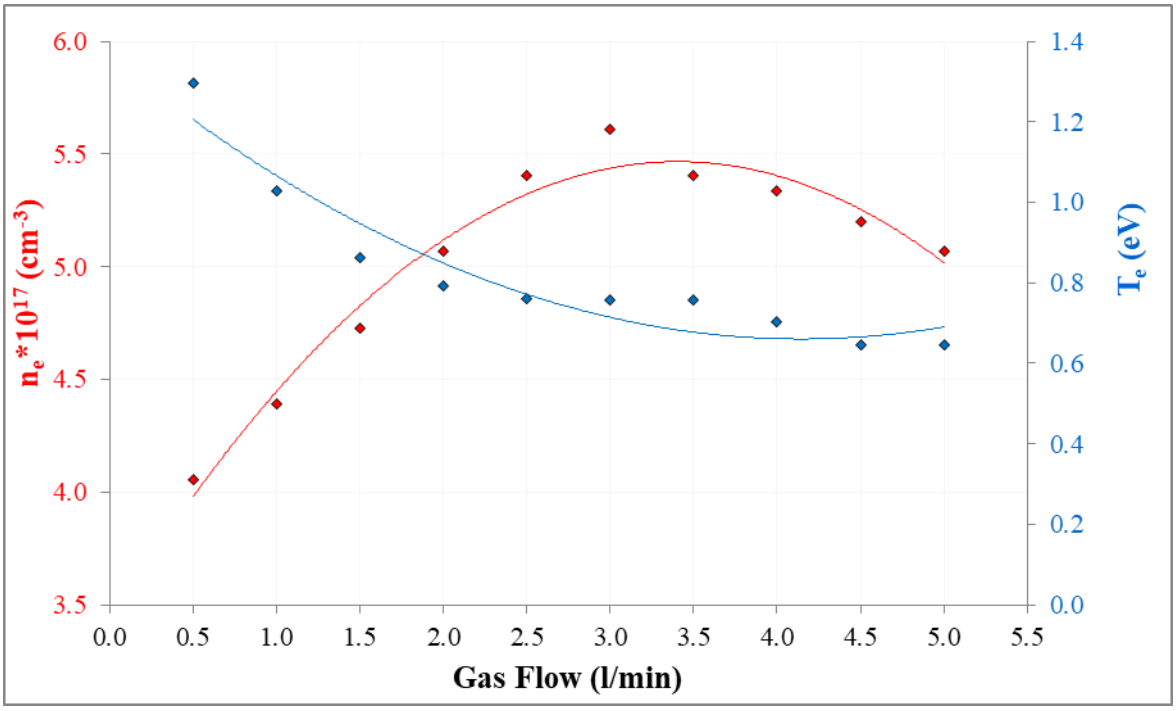


Figure 5: The Relationship between Electron Temperature and Electron Density as a Flow Function

As gas flow rate increases, there are more collisions between the gas atoms and the electrons. Due to the enhanced energy transfer from the electrons to the gas particles as a result of such collisions, the gas's temperature is increased while the electrons' temperature is decreased. A large part of the excitation and ionization regarding ionic and atomic species in argon plasma is also assumed to be played by electron impact. As gas flow rate rose, the high-energy tail of the electron energy distribution function shifted to lower energies. Stepwise ionization consequently lead to an increase in electron density with flow rate, which lowers direct ionization, which is brought on by energetic electrons directly interacting with gas atoms [12,13]. The n_e, T_e, f_p, λ_D, and N_D for Ar gas at a variety of the flow rates are shown in Table 1. The results of plasma parameters (T_e, λ_D) that had shown a reduction with the increase in flow rate utilized for producing the criteria plasma. n_e and f_p, on the other hand, showed the reverse (decreasing) pattern. This is consistent with findings of a previous research [14].

Table 1: The Plasma Parameters for Argon Gas with Changed Flow Rates (L/min)

Gas Flow (L/min)	Te (eV)	FWHM (nm)	n_e*10^{17} (cm^{-3})	f_p (Hz) $*10^{12}$	λ_D $*10^{-6}$(cm)	N_d
0.5	1.296	0.600	4.054	5.718	1.328	4
1.0	1.028	0.650	4.392	5.951	1.137	3
1.5	0.863	0.700	4.730	6.176	1.004	2
2.0	0.794	0.750	5.068	6.393	0.930	2
2.5	0.759	0.800	5.405	6.602	0.881	2
3.0	0.757	0.830	5.608	6.725	0.863	2
3.5	0.759	0.800	5.405	6.602	0.881	2
4.0	0.702	0.790	5.338	6.561	0.852	1
4.5	0.645	0.770	5.203	6.477	0.827	1
5.0	0.645	0.750	5.068	6.393	0.839	1

Conclusions

A cold plasma system operating at atmospheric pressure was built and designed using argon gas with a high voltage equipment, a fixed applied voltage of 12 kV was used to generate argon plasma at variable gas flow values of (0.5-5) *l/min*. The system was diagnosed by (OES) and different peaks were obtained for argon gas and nitrogen gas. The results showed obtaining the highest peak of argon gas at the wavelength of 763.51 nm with some other peaks along the spectral line. The results showed the direct effect of increasing the gas flow on the measured plasma parameters values. Where the temperature and the density of the electron at the flow of argon gas 0.5 *l/min* was

1.296 eV and 4.054×10^{17} cm^{-3} respectively, while at the gas flow of 5 *l/min* was 0.645 eV and 5.068×10^{17} cm^{-3}. The results showed that there is a direct proportion to the electron density with increase in Ar gas flow rates and an inverse proportion to the electron temperature. This leads us to the conclusion that an increase in the gas flow rate greatly affects the plasma parameters.

References

Ziuzina, D., Patil, S., Cullen, P.J., Keener, K.M., & Bourke, P. (2013). Atmospheric cold plasma inactivation of E scherichia coli in liquid media inside a sealed package. *Journal of applied microbiology*, *114*(3), 778-787.

Murbet, H., & ALameer, H. (2016). Effect of gas flow rate on plasma temperature and electron density. *Iraqi Journal of Physics*, *12*, 14-25.

Boudam, M.K., Moisan, M., Saoudi, B., Popovici, C., Gherardi, N., & Massines, F. (2006). Bacterial spore inactivation by atmospheric-pressure plasmas in the presence or absence of UV photons as obtained with the same gas mixture. *Journal of Physics D: Applied Physics*, *39*(16), 3494-3507.

Noriyasu, O., Abdur, M., Hiroshi, U., Shuichi, T., & Yoshihiko, U. (2006). Plasma and Fusion Research, *1*, 1-28.

Devia, D.M., Rodriguez-Restrepo, L.V., & Parra, E.R. (2015). Methods employed in optical emission spectroscopy analysis: a review. *Ingeniería y ciencia*, *11*(21), 239-267.

Hamed, S.S. (2005). Spectroscopic determination of excitation temperature and electron density in premixed laminar flame. *Egypt. J. Solids*, *28*(2), 349-357.

Sansonetti, J.E., & Martin, W.C. (2005). Handbook of basic atomic spectroscopic data. *Journal of physical and chemical reference data*, *34*(4), 1559-2259.

Qiuping, Z., Cheng, C., & Yuedong, M. (2009). Electron density and temperature measurement by Stark Broadening in a cold argon arc-plasma jet at atmospheric pressure. *Plasma Science and Technology*, *11*(5), 560-563.

Dezhi, X., Ch. Cheng, Ie. Shen, L. Yan, X. Hongbing, Shu Xingsheng, M. Yuedong, Li Jiangang, P.K. Ch. (2014). *Physics of Plasma*, *21*, 53510-53517.

Hammad, R.H., Qusay, A.A., & Aws, F.R. (2015). *International Journal of Current Engineering and Technology, 5*(6), 2347-5161.

Tu, X., Chéron, B.G., Yan, J.H., & Cen, K.F. (2007). Electrical and spectroscopic diagnostic of an atmospheric double arc argon plasma jet. *Plasma Sources Science and Technology*, *16*(4), 803-812.

Sansonetti, J.E., & Martin, W.C. (2005). Handbook of basic atomic spectroscopic data. *Journal of physical and chemical reference data*, *34*(4), 1559-2259.

Moon, S.Y., Choe, W., Uhm, H.S., Hwang, Y.S., & Choi, J.J. (2002). Characteristics of an atmospheric microwave-induced plasma generated in ambient air by an argon discharge excited in an open-ended dielectric discharge tube. *Physics of Plasmas*, *9*(9), 4045-4051.

Aadim, K.A. (2019). Spectroscopic study the plasma parameters for SnO_2 doped ZnO prepared by pulse Nd: YAG laser deposition. *Iraqi Journal of Physics*, *17*(42), 125-135.